Journal of Computer-Aided Molecular Design **17:** 583–595, 2003.

Computational studies of new potential antimalarial compounds – Stereoelectronic complementarity with the receptor

César Portela[a], Carlos M.M. Afonso[a], Madalena M.M. Pinto[a] & Maria João Ramos[b,*]
[a]*Centro de Estudos de Química Orgânica, Fitoquímica e Farmacologia da Universidade do Porto – Faculdade de Farmácia, Rua Aníbal Cunha, 164, 4050-047 Porto, Portugal;* [b]*Requimte – Departamento de Química, Faculdade de Ciências, Universidade do Porto – Rua do Campo Alegre, 687, 4169-007 Porto, Portugal*

Received 22 April 2003; accepted in revised form 15 August 2003

Key words: antimalarial activity, DFT, docking, hematin aggregation, malaria, quantum mechanics, stereoelectronic properties, xanthones

Summary

One of the most important pharmacological mechanisms of antimalarial action is the inhibition of the aggregation of hematin into hemozoin. We present a group of new potential antimalarial molecules for which we have performed a DFT study of their stereoelectronic properties. Additionally, the same calculations were carried out for the two putative drug receptors involved in the referred activity, i.e., hematin μ-oxo dimer and hemozoin. A complementarity between the structural and electronic profiles of the planned molecules and the receptors can be observed. A docking study of the new compounds in relation to the two putative receptors is also presented, providing a correlation with the defined electrostatic complementarity.

Introduction

Malaria is one of the major health problems in the world. It is estimated that 40% of the population of our planet is exposed to the disease, with a prevalence of the order of 300–500 million clinical cases and 2 million deaths each year [1, 2]. In addition, the available antimalarial drugs are losing their efficacy, due to the development of resistance by the parasite [3–5]. The continuing spread of drug-resistant malaria imposes a need for the search of new antimalarial compounds, which could constitute an alternative to the currently used drugs [3–5].

The malaria parasite has a limited capacity for *de novo* amino acid synthesis, needed to acquire some of these essential nutrients to survive. The essential amino acids are obtained from human hemoglobin proteolysis [6]. This digestion of hemoglobin releases the heme moiety, which oxidizes to hematin, also known as ferriprotoporphyrin IX (Figure 1) [6]. Free hematin is toxic to the parasite, damaging cellular metabolism by inhibition of enzymes, causing the peroxidation of membranes and originating the production of oxidative free radicals in the acidic environment of the digestive vacuole [6]. Lacking the heme oxygenase that vertebrates use for heme catabolism, plasmodial species detoxify by sequestering this by-product into a chemically inert crystal [6]. The product formed, hemozoin, is an aggregate of several units of hematin linked by carboxylate-iron(III) and carboxylate–carboxylate coordinated bonds [7–9].

The referred detoxification process can be used as a target for antimalarial therapy [10–12]. Several antimalarial compounds interfere in this metabolical pathway by associating with a derivative form of hematin, avoiding the aggregation of this porphyrin [13–15]. The death of the parasite arises as a consequence of the toxicity of the free hematin [16–21]. The most likely is that the drug–receptor association occurs between the antimalarial molecule and one or several units of a μ-oxo-dimer of hematin [13–15, 22–26]. The hematin μ-oxo-dimer is a complex of two molecules of hem-

*To whom correspondence should be addressed. E-mail: mjramos@fc.up.pt

atin connected by an oxygen bridge between the two iron atoms [9].

The hemozoin structure can also constitute a probable receptor, with the antimalarial drug action arising from surface adsorption on the actively growing surfaces of hemozoin crystallites [8]. This adsorption phenomenon would limit the uptake of new hematin subunits, originating a toxic action against the parasite [8]. The establishment of hemozoin as another possibility for a drug receptor was due to its structural definition by high-resolution X-ray powder diffraction [8].

A part of the present study is an assessment of the structural and electronic properties of these two putative receptors: hematin μ-oxo-dimer and hemozoin structure.

Considerable data now support the hypothesis that antimalarial 4-aminoquinolines like chloroquine prevent the formation of hemozoin, inhibiting parasite growth [25–35]. Drugs like mefloquine or halofantrine also present the ability of inhibiting this aggregation phenomenon [25, 26, 30–32]. Other studies concerning hydroxylated xanthones have shown that these compounds present antimalarial activity, by the same molecular mechanism [36–39].

The observation of the stereoelectronic characteristics of these active compounds [36-48], and the definition and interpretation of the stereoelectronic properties of the two putative receptors involved in their action served as a base for the rational planning of new xanthone derivatives, namely the proposed chlorinated xanthones (Figure 2). The use of chlorine atoms as substituents was due to the relevance of this halogen in the activity of 4-aminoquinolines [25–35] and for its known electron withdrawing behavior. The introduction of an aminated side chain serves the pharmacokinetic purpose of allowing the accumulation of the compounds inside the *Plasmodium* vacuole [40–44, 49, 50]. This effect is essential for the development of an antiplasmodial action in active compounds like 4-aminoquinolines, halofantrine or mefloquine. This vacuole accumulation is a consequence of the protonation of the nitrogen atoms due to a pH in the range of 4.5 to 5.5 [40–44, 49, 50]. The resistance overcoming presented by 4-aminoquinolines with a side chain of two carbons between the nitrogen atoms dictated its application in the new chloroxanthones [43, 44]. The studied structures are divided in three classes (Figure 2). Class A corresponds to intermediates of the final compounds that can also present an inhibitory action over hematin aggregation. Class

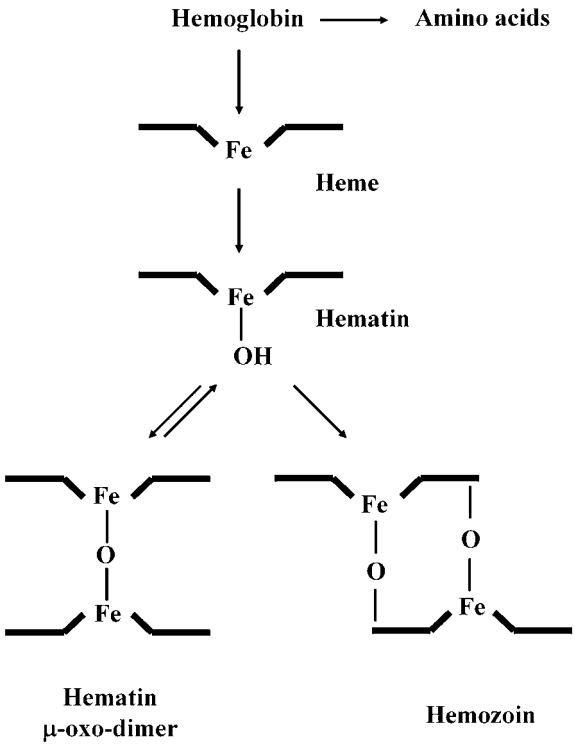

Figure 1. Schematic representation of heme detoxification pathway of the malaria parasite.

B structures were modelled to evaluate the influence of the amino group in the electrostatic profile. Class C corresponds to the final compounds, which present pharmacokinetic properties that, together with their stereoelectronic characteristics, can develop a more efficient antimalarial action.

The study of the stereoelectronic properties was carried out using Density Functional Theory [51–53]. This method conjugates the possibility of introducing the concept of electronic correlation in the calculations, with a computational effort similar to the Hartree–Fock methods.

The docking study was performed using an automated procedure consisting of the application of the GOLD, genetic algorithm [54–57], using both scoring functions, Goldscore and Chemscore [54–59]. This algorithm was designed to determine the docking position of ligands in relation to the receptor [54–57]. GOLD constitutes one of the most respected programs for docking studies [60, 61]. The application of this method was performed with the aminated chloroxanthones in the protonated state that occurs at the pH conditions inside the parasite vacuole [49, 50]. The

receptors were used with one of the carboxylic groups deprotonated, for each hematin subunit, as *in vivo.*

Materials and methods

Geometry optimizations and energy calculations for the new xanthonic compounds (neutral and protonated forms), chloroquine, mefloquine and halofantrine were performed at an *ab initio* quantum mechanical level by using Density Functional Theory (DFT) with the Becke3-Lee-Yang-Parr (B3LYP) functional [51–53], and the 6-31G(d) basis set [62–65]. This basis set was used due to the known fact that larger basis sets give very small additional corrections to the geometries, and their use is hence considered unnecessary from a computational view [62–65]. Compounds 1C to 12C were submitted to a conformational search using the CHARMM force field [66, 67]. This study was performed due to the conformational flexibility presented by the existence of a linear side chain.

The three-dimensional structure of the μ-oxo-dimer of hematin had to be modeled, because it has not been resolved experimentally. A conformational search was first performed using the CHARMM force field [66, 67] to find out the most likely position of the porphyrin subunits to each other, as well as the propionic and vinyl substituents. A geometry optimization was then carried out with the AM1(d) semi-empirical method [68, 69] and the resulting neutral structure was further submitted to a single point calculation using DFT with the B3LYP functional and the 6-31G(d) basis set.

The three-dimensional structure of the hemozoin dimer was obtained from the Cambridge Crystallographic Database [8]. The structure was further submitted to a single point calculation using DFT with the B3LYP functional and the 6-31G(d) basis set.

Both hemozoin and the μ-oxo-dimer of hematin show a spin state of $^5/_2$, as determined by Mössbauer spectroscopy [70–73]. This was the value considered in the calculations performed on the hematin complexes.

All DFT calculations were performed with the Gaussian 98 package [74].

Molecular Electrostatic Potential (MEP) surfaces were drawn using the CUBEGEN utility present in Gaussian 98 [74], applied to the optimized geometries of all molecules. These MEP isoenergy contours were generated in the range of −50 to 50 kcal/mol, superimposed onto a surface of constant electron density (0.0002 e/bohr^3), to provide a measure of the electrostatic potential at roughly the van der Waals surface of the molecule. This color-coded surface provides a measure of the overall size of the molecule as well as the location of negative or positive electrostatic potentials. The regions of positive electrostatic potential indicate excess positive charge, leading to repulsion of the positively charged test probe, while regions of negative potential indicate areas of excess negative charge, leading to attraction of the positively charged test probe.

Three-dimensional surfaces of molecular electrostatic potential at the constant values of −5 and −10 kcal/mol were generated to determine the profile of the electrostatic potential of a molecule when approaching the receptor.

The calculation results obtained in vacuum or using the continuum (SCPCM model as implemented in Gaussian 98 [74]) to simulate the aqueous environment did not differ, originating identical surfaces.

The visualization of all quantum calculations results was performed with Molekel 4.2 [75].

The docking procedure was performed with GOLD, Genetic Optimisation for Ligand Docking, using both scoring functions available [54–57]. The Goldscore function is defined to predict ligand binding positions [54–57], whereas the Chemscore function is developed by regression against ligand–receptor binding free energies [58, 59]. The work was performed in the standard default settings for the best possible predictive accuracy, with 10 docking runs for each ligand, without early termination. All atoms of both receptors have been supplied as the cavity. Visualisation of docking results was performed with DS ViewerLite from Accelrys [76].

Results and discussion

The proposed structures (Figure 2) were modelled with the definition of the optimised geometry, the distribution of the electrostatic potential, and the docking position in the two possible receptors. They present a stereoelectronic profile comparable to compounds like mefloquine or hydroxylated xanthones. Their electrostatic behavior is complementary to the putative receptors described. The intended electronic profile is accomplished by the inductive effect of the chlorine atoms and the electron withdrawing behavior of the xanthonic carbonyl group.

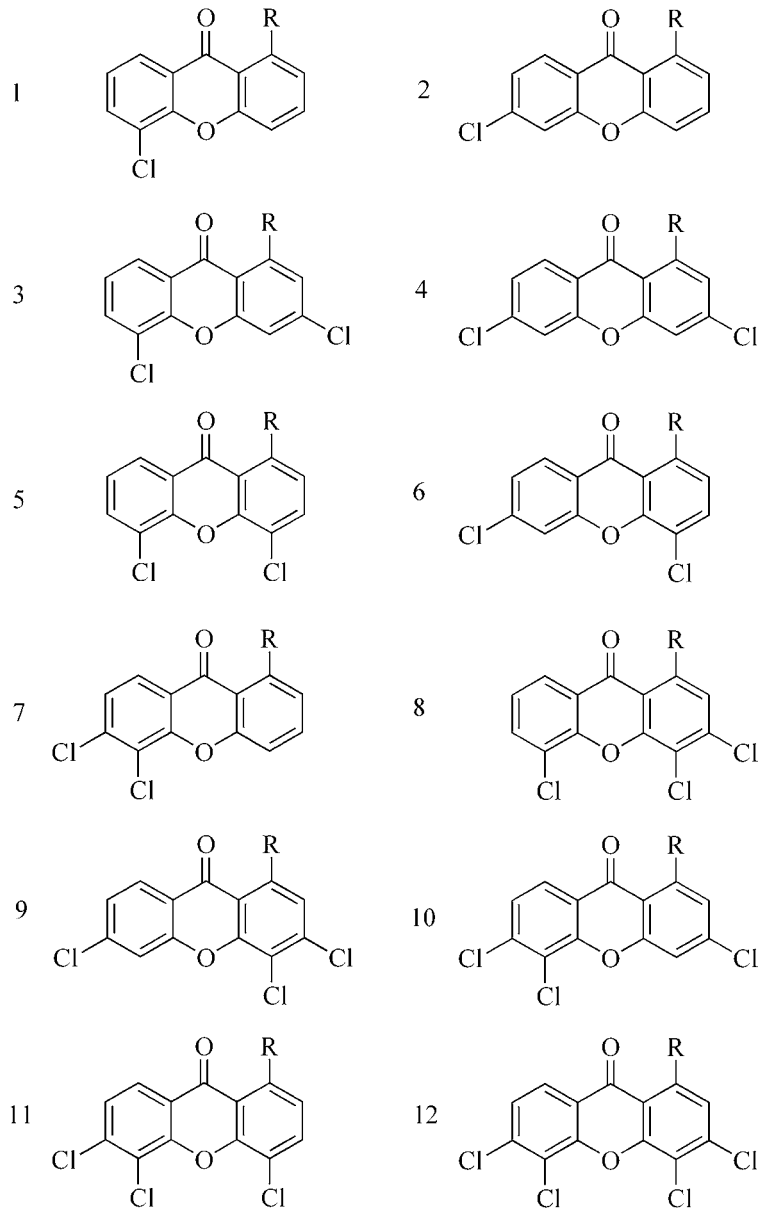

1A to 12A: R=Cl

1B to 12B: R=NH2

1C to 12C: R= HN–N

Figure 2. New potential antimalarial xanthonic derivatives.

Molecular Electrostatic Potentials

The three-dimensional Molecular Electrostatic Potential (MEP) maps superimposed onto total electron density account for the interpretation of short-range interactions between molecules. At each point of the map, the electrostatic potential expresses the value of the electrostatic energy of interaction with a unitary positive charge. The three-dimensional MEP isosurfaces can account for the interpretation of long-range interactions [77]. This representation helps to understand how interactions between a drug and its receptor can occur.

The three-dimensional MEP map superimposed onto total electron density of the hematin μ-oxo-dimer exhibits a profile with values of potential ranging from −50 kcal/mol to 30 kcal/mol (Figure 3). The most negative potential is located on the position occupied by the iron atoms and the tetrapyrrol system, with the most positive potential found at the surrounding area. The carboxyl oxygen atoms also present negative electrostatic potential (Figure 3).

The electrostatic potential isosurfaces at values of −10 and −5 kcal/mol show a large negative surface centered on the dimer (Figure 3), corresponding to the iron, the oxygen bridge and the pyrrolic nitrogen atoms system. The area around these surfaces corresponds to a positive electrostatic potential. The carboxylic groups present a negative potential located on the oxygen atoms, with a positive potential placed on the carbon and the hydrogen atoms.

Observing the distribution of electrostatic potential in this receptor, we can define a possibility of association, with an active molecule presenting a complementary electrostatic profile. The central point of positive potential of the active molecule would approach the negative central zone of the hematin dimer, and the peripheral points of negative potential would move towards the peripheral positive area of this receptor [78]. As a consequence, the iron atoms would not be available to establish a coordination bond with a propionic chain from another hematin unit, inhibiting the formation of hemozoin.

The observation of the MEP map superimposed onto total electron density of the hemozoin dimer denotes the presence of a negative value of potential at the points of carboxylate-iron(III) coordination, with a peripheral positive potential (Figure 4). The MEP isosurfaces at values of −10 and −5 kcal/mol are in accordance with the previously stated facts, showing one of the subunits possessing a more distributed negative potential. The possibilities of approach and association between the hematin μ-oxo-dimer putative receptor and an active compound referred to above are also applicable to the hemozoin case.

The antimalarial compounds can therefore act by stabilising the receptor due to the electrostatic interactions determined by their complementary electronic profiles, avoiding a further uptake of hematin in the aggregation phenomenon that leads to the crystal form of hemozoin.

The observation of the electrostatic profiles of 4-aminoquinolines, mefloquine, halofantrine or active hydroxylated xanthones, which interfere with the hematin aggregation pathway, is in accordance with the possibility of drug–receptor association presented (Figure 5). These compounds present a positive potential placed over part of the aromatic rings. The existence of peripheral bulks of negative potential can also be observed.

The new proposed xanthone derivatives (Figure 2) correlate with all this information, and can interact with the two putative receptors in the same way of known active compounds, presented before. The electrostatic characteristics are accomplished by the inductive effect of the chlorine atoms and the electron withdrawing behavior of the carbonyl group.

MEPs superimposed onto total electron density and three-dimensional electrostatic potential isosurfaces at −10 and −5 kcal/mol are presented in Figures 6 and 7, for examples belonging to each of the three classes A, B and C. All the chlorinated xanthone derivatives show a positive potential placed at the center of the ring system, being the negative potential located in the carbonyl oxygen and chlorine atoms. The presence of higher positive values of potential connected with the aromatic rings can lead to a better antimalarial activity, by increasing the susceptibility to nucleophilic attacks on the aromatic rings of this group of compounds [40, 45–48]. This happens as a consequence of increasing the number of chlorine atoms.

The three-dimensional MEP isosurfaces at values of −10 and −5 kcal/mol for all compounds show a bulk of negative potential placed in the carbonyl oxygen (Figure 7). The increasing number of chlorine substituents leads to broader bands of negative potential, placed peripherally to the aromatic rings system.

The positive value of potential in the aromatic ring does not diminish due to the introduction of an aminated side chain in position 1. On the contrary, the

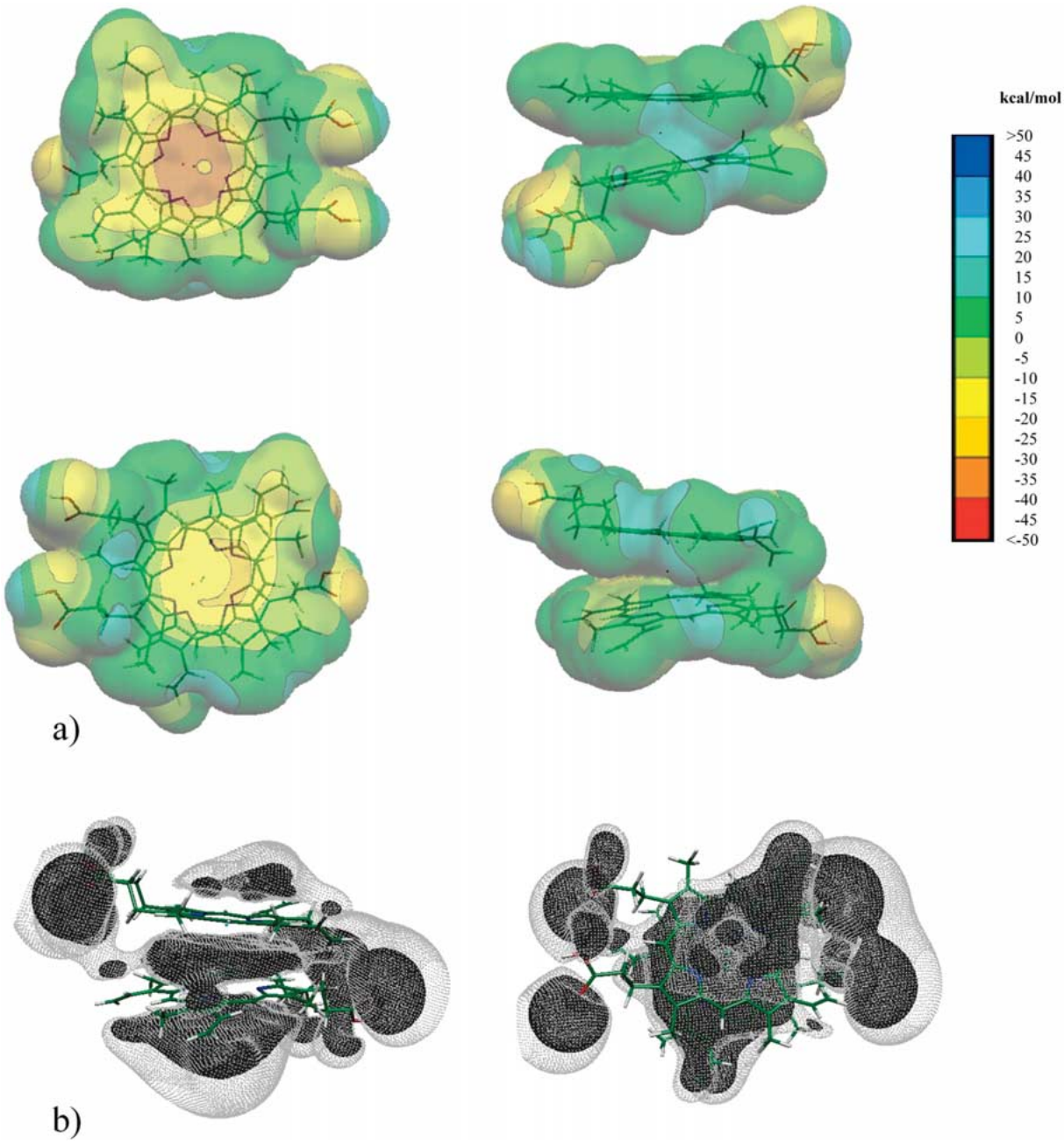

Figure 3. (a) MEPs superimposed onto total electron density at a value of 0.0002 e/bohr^3 for the hematin μ-oxo-dimer; (b) three-dimensional electrostatic potential isosurface at −10 kcal/mol (dark grey) and −5 kcal/mol (light grey - dots) for the hematin μ-oxo-dimer.

negative potential over the carbonyl oxygen diminishes, increasing its intensity over the chlorine atoms (Figures 6 and 7). To determine if this alteration was due to the side chain or only because of the direct influence of the amino group directly linked to the aromatic moiety, the same calculations were performed over structures differing only by the introduction of an amino group in position 1. The electrostatic profiles for compounds with the amino group and with the aminated side chain are not significantly different. This fact points out to the amino group directly attached as an intervenient in the definition of this

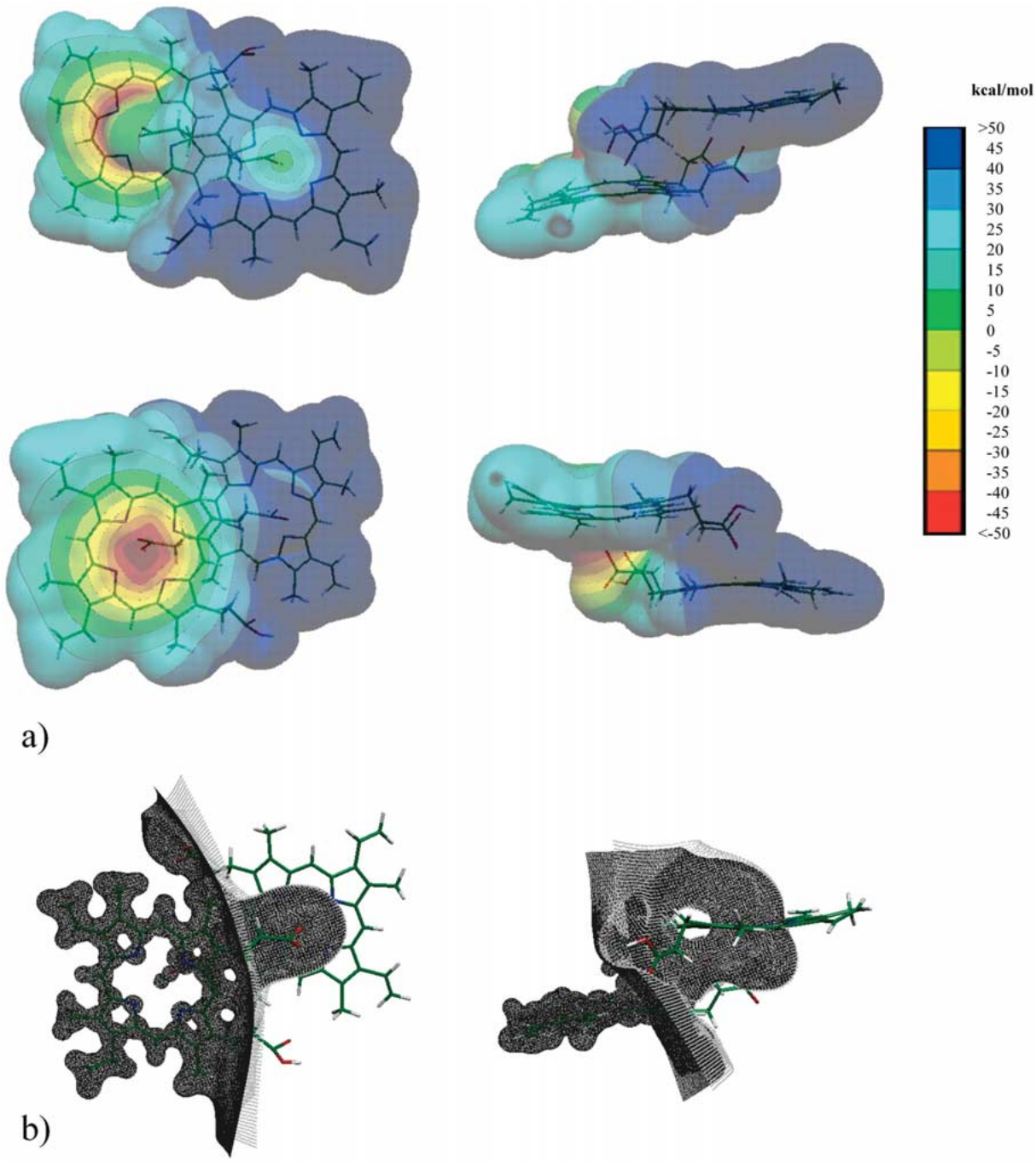

Figure 4. (a) MEPs superimposed onto total electron density at a value of 0.0002 e/bohr^3 for the hemozoin dimer; (b) three-dimensional electrostatic potential isosurface at −10 kcal/mol (dark grey) and −5 kcal/mol (light grey - dots) for the hemozoin dimer.

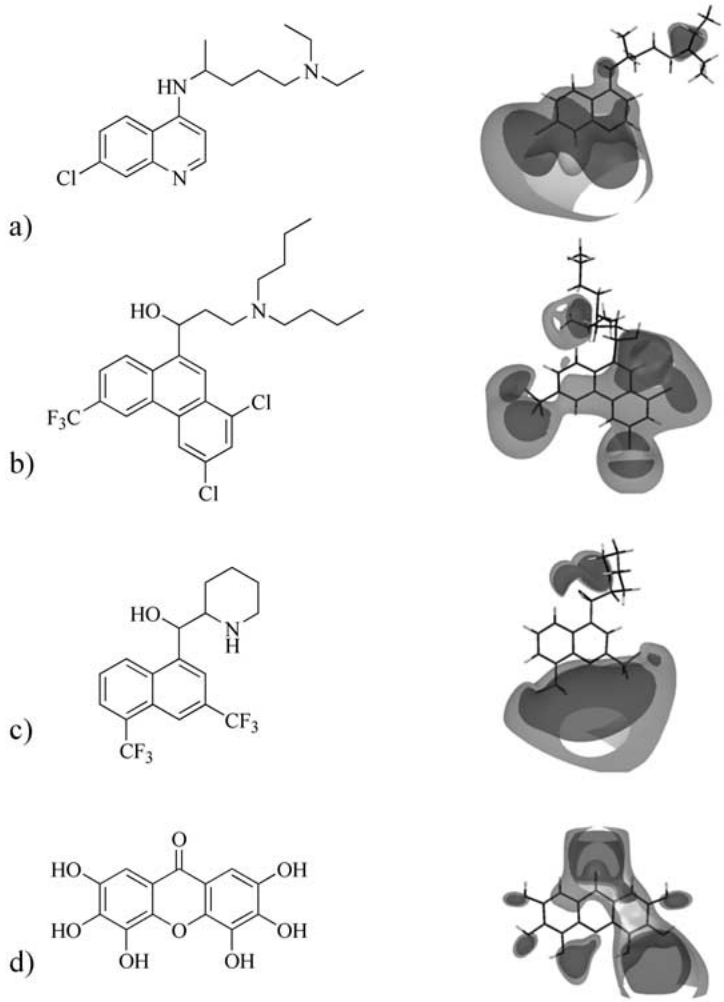

Figure 5. Three-dimensional electrostatic potential isosurfaces at −10 kcal/mol (dark grey) and −5 kcal/mol (light grey) for: (a) Chloroquine, (b) Halofantrine, (c) Mefloquine, and (d) 2,3,4,5,6,7-Hexahydroxyxanthone.

electronic behavior. The aminated side chain will allow a better accumulation of the compounds inside the acidic vacuole of the parasite, due to an inevitable protonation.

The more intense bulks of negative potential together with a more positive potential located in the aromatic rings can reinforce the attraction for the receptor and, consequently, increased activity.

It is important to note that we have just used MEPs to postulate different forms of interaction between the putative receptors and the different ligands. However, the MEP is not a static entity, i.e., it changes as the ligand approaches the receptor site just as does the respective electron density. Nevertheless, the analysis of the isolated MEPs is useful to suggest the way the ligand approaches the receptor, and therefore predict the overall picture that a successful ligand, as far as aggregation to the receptor is concerned, should have.

Docking

The docking study was carried out to predict how the potential antimalarial molecules would bind to both putative receptors, by using a non-deterministic sampling method. The GOLD algorithm performs a stochastic search for preferred orientation and conformation of the ligand in relation to the receptor [61].

The GOLD algorithm gave good results in the investigation of the binding of several antimalarial compounds to the putative drug receptors involved in the hematin aggregation process [79]. The results

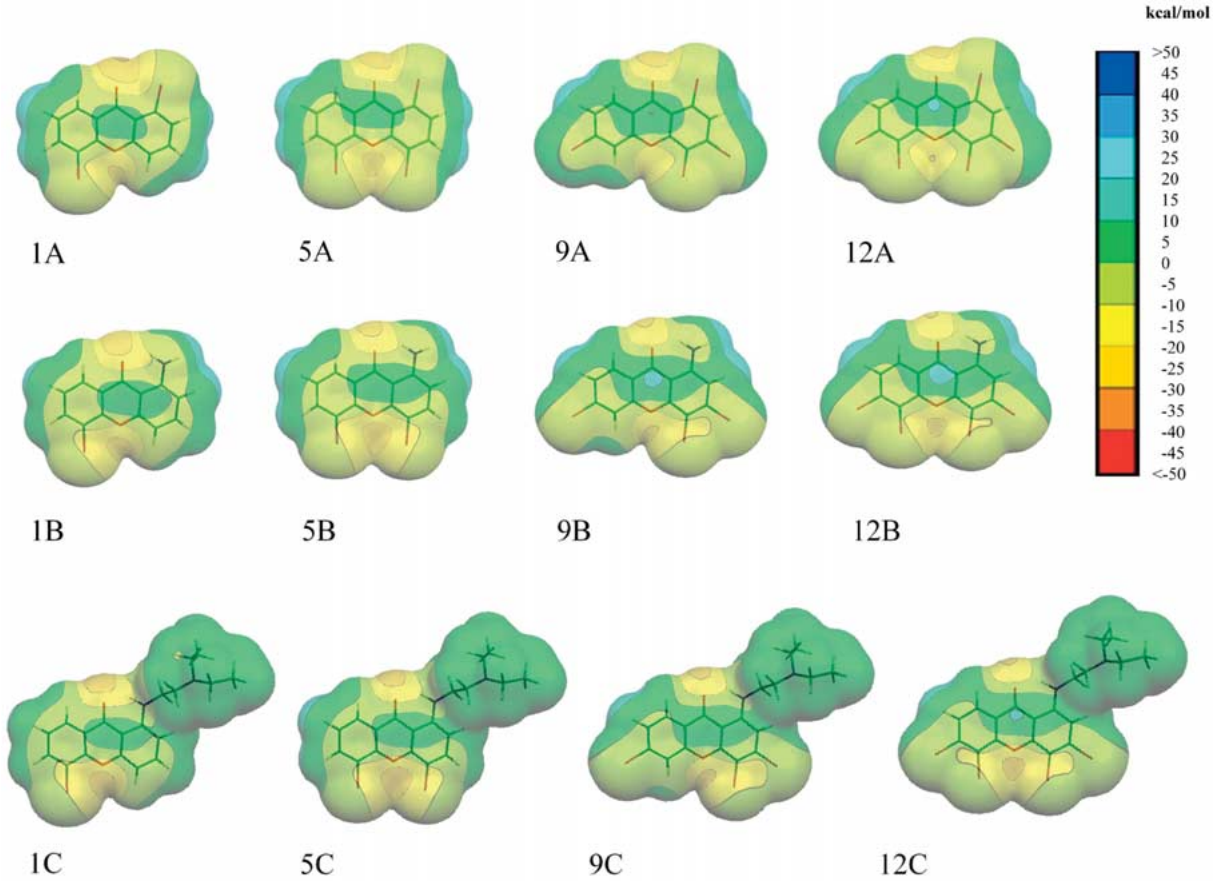

Figure 6. MEPs superimposed onto total electron density at a value of 0.0002 e/bohr^3 for some examples of the new compounds (see Figure 2).

obtained correlated well with the complementarity of electrostatic potentials for all compounds under study [79]. The results obtained for chloroquine and quinine were comparable to the results obtained by nuclear magnetic resonance [79].

The calculations were performed on the receptors in the deprotonated form, as *in vivo*. The molecules used were 1A to 12A and 1C to 12C. Class B was not used in the docking studies due to the fact that these structures were modelled only to study the impact in the electrostatic profile caused by the substituent in position 1. The aminated compounds 1C to 12C were studied in their protonated form (Figure 2). The results correspond to the best-scored solutions of docking for each new structure. Both scoring functions available in GOLD were used. The results obtained with Goldscore and Chemscore correlate for most compounds.

The association with the hematin μ-oxo-dimer gave similar results among all compounds, corresponding to the electrostatic behavior previously defined (Figure 8a). The central aromatic area of the ligand, with positive electrostatic potential, interacts with the negative central zone of the hematin dimer. The peripheral negative potential of the ligand interacts with the peripheral positive area of this μ-oxo-dimer receptor.

The docking with hemozoin presented results coherent with the concept of complementarity of electrostatic potentials, although different from the ones we expected. It would have been predictable that they would associate with the hematin units present in the hemozoin dimer in the same way that happened with the hematin μ-oxo-dimer, covering the iron atoms and avoiding the consequent coordination with the propionic chain of the other hematin. This result was obtained only for compounds 5C and 12C, with the scoring function Chemscore (Figure 8b). The other compounds associated in the same way as presented in Figures 8c and 8d. Compounds 1C to 4C and 6C to 11C, presenting an aminated side chain, docked

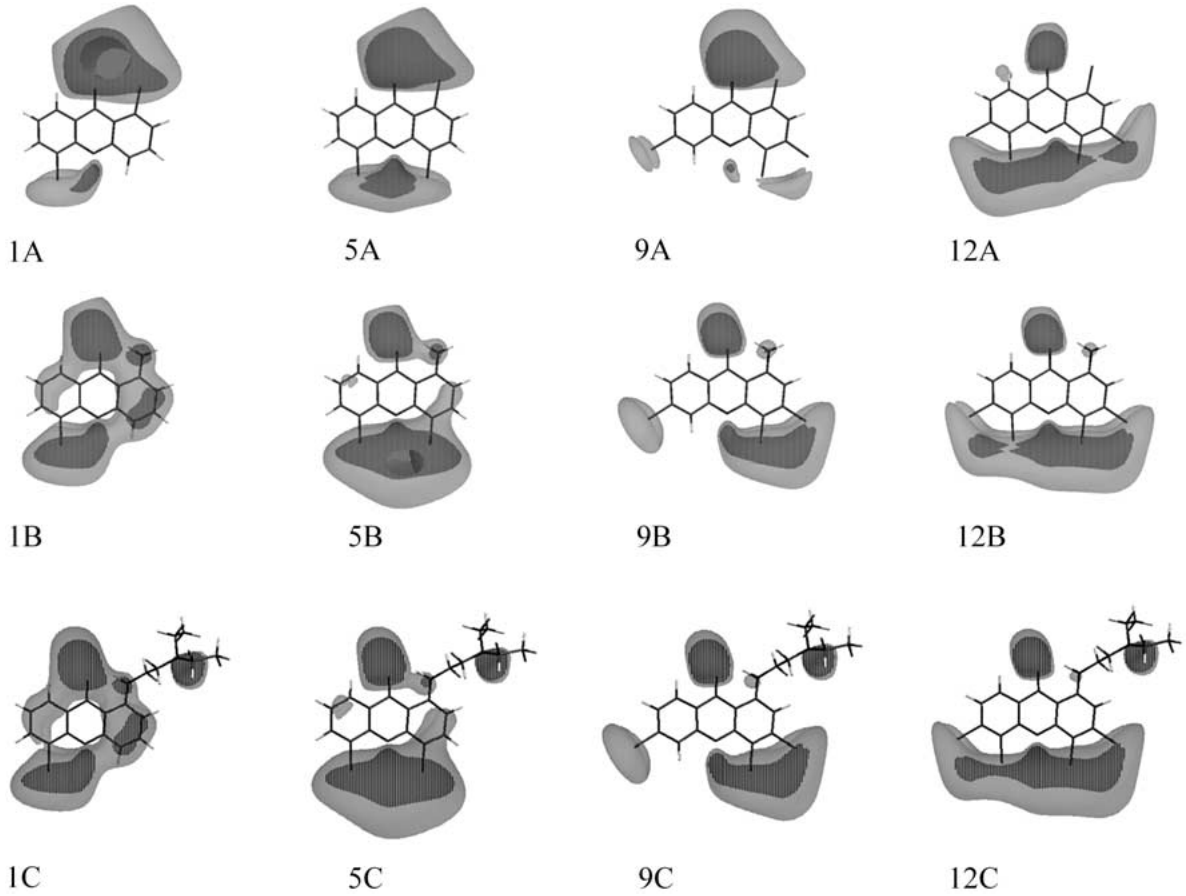

Figure 7. Three-dimensional electrostatic potential isosurfaces at −10 kcal/mol (dark grey) and −5 kcal/mol (light grey) for some examples of the new compounds (see Figure 2).

with the area of negative potential over the carbonyl group approaching the positive area surrounding the carboxylate-iron(III) system (Figure 8c). Compounds 1A to 12A also originated solutions with the area of negative potential over the carbonyl group approaching the positive area surrounding the carboxylate-iron(III) system. Conformations with the negative potential over the chlorine atoms associating with the positive area surrounding the carboxylate-iron(III) system are also present (Figure 8d).

Conclusions

This work presents new potential antimalarial compounds and their stereoelectronic features. Stereoelectronic models of the hematin μ-oxo-dimer and hemozoin have been developed also. Since stereoelectronic features seem to control primarily the inhibitory activity against hematin aggregation, the recognition of the stereoelectronic characteristics of the receptor were very helpful in the development of the new potential antimalarial structures. Complementarity between the putative receptors and related antimalarial drugs is observed. This fact constituted a basis for the planning and theoretical study of new potential antimalarial molecules.

The synthesis and antimalarial activity evaluation of these new xanthone derivatives are underway.

Acknowledgements

FCT (I&D N^{o}226/94), POCTI (QCA III), FEDER and PRAXIS XXI Recipient of PhD grant from FCT: César Portela (SFRH/BD/3036/2000). M.J. Ramos thanks the NFCR for financial support.

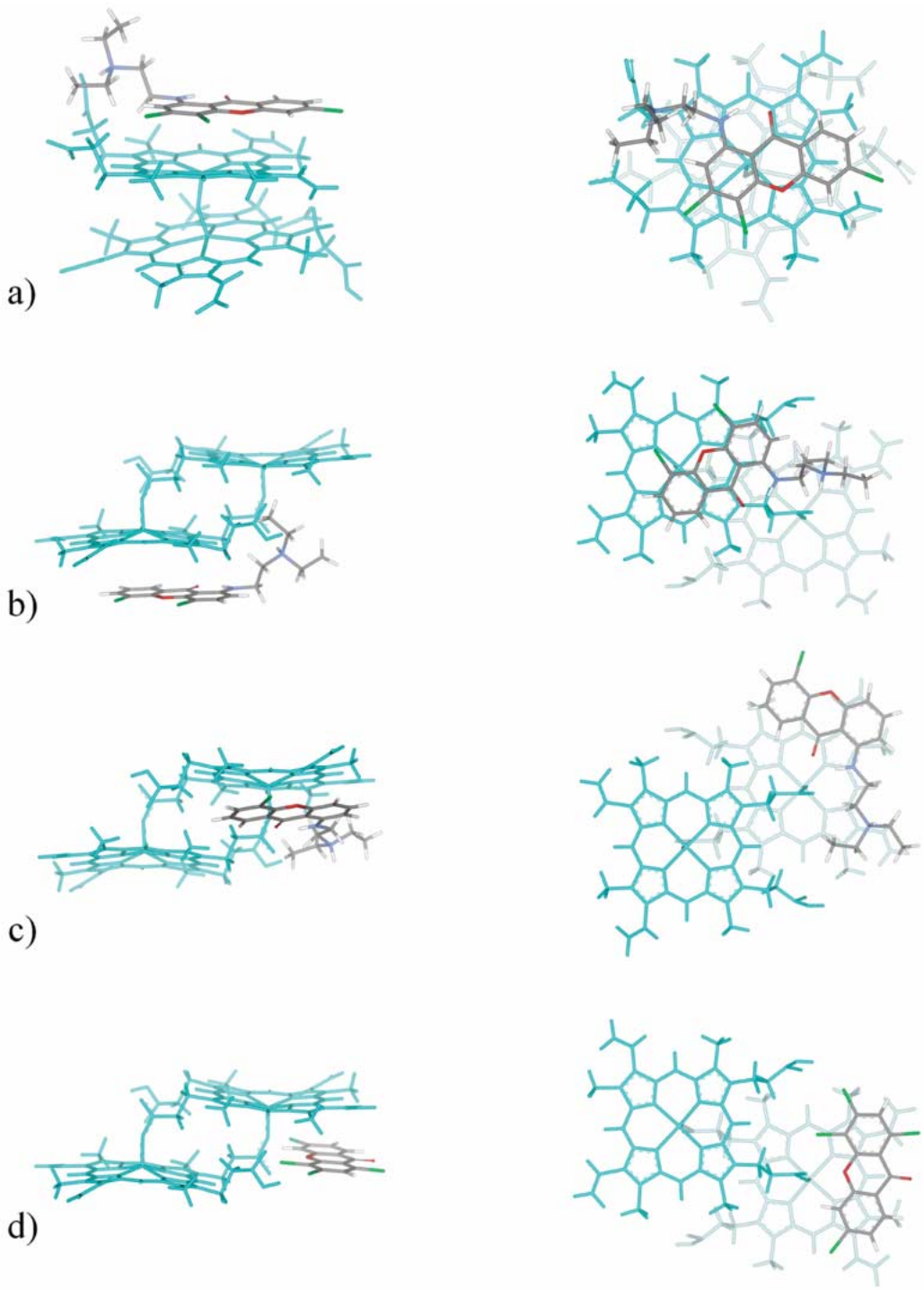

Figure 8. Docking results for: (a) Compound 9C over hematin μ-oxo-dimer, with Chemscore; (b) Compound 5C over hemozoin, with Chemscore; (c) Compound 1C over hemozoin, with Goldscore; (d) Compound 9A over hemozoin, with Goldscore.

References

1. Winstanley, P.A., Parasitol. Today, 16 (2000) 146.
2. Greenwood, B.M., Parasitol. Today, 13 (1997) 90.
3. Koella, J.C., Parasitol. Today, 14 (1998) 360.
4. Bray, P.G., Mungthin, M., Ridley, R.G. and Ward, S.A., Mol. Pharm., 54 (1998) 170.
5. Ginsburg, H. and Krugliak, M., Drug Resistance Updates, 2 (1999)180.
6. Francis, S.E., Sullivan, D.J., Jr. and Goldberg D.E., Annu. Rev. Microbiol., 51 (1997) 97.
7. Blauer, G. and Akkawi, M.J., Inorg. Biochem., 66 (1997) 145.
8. Pagola, S., Stephens, P.W., Bohle D.S., Kosar, A.D. and Madsen S.K., Nature, 404 (2000) 307.
9. Bohle, D.S., Dinnebier, R.E., Madsen, S.K. and Stephens, P.W., J. Biol. Chem., 272 (1997) 713.
10. Dorn, A., Stoffel, R., Matile, H., Bubendorf, A. and Ridley, R.G., Nature, 374 (1995) 269.
11. Fitch, C. D. and Chou, A.C., Antimicrob. Agents Chemother., 41 (1997) 2461.
12. Zhang, J., Krugliak, M. and Ginsburg, H., Mol. Biochem. Parasitol., 99 (1999) 129.
13. Vippagunta, S.R., Dorn, A., Ridley, R.G. and Vennerstrom, J.L., Biochim. Biophys. Acta, 1475 (2000) 133.
14. Moreau, S., Perly, B. and Biguet, J., Biochimie, 64 (1982) 1015.
15. Moreau, S., Perly, B., Chachaty, C. and Deleuze, C., Biochim. Biophys. Acta, 840 (1985) 107.
16. Chou, A.C. and Fitch, C.D., J. Clin. Invest., 66 (1980) 856.
17. Orjih, A.U., Banyal, H.S., Chevli, R. and Fitch, C.D., Science, 214 (1981) 667.
18. Ginsburg, H. and Demel, R.A., Biochim. Biophys. Acta, 772 (1983) 316.
19. Hebbel, R.P. and Eaton, J.W., Semin. Hematol., 26 (1989) 136.
20. Ginsburg, H., Famin, O., Zhang, J. and Krugliak, M., Biochem. Pharmacol., 56 (1998) 1305.
21. Sugioka, Y. and Suzuki, M., Biochim. Biophys. Acta, 1074 (1991) 19.
22. Chou, A.C., Chevli, R. and Fitch, C.D., Biochemistry, 19 (1980) 1543.
23. Egan, T.J., Mavuso, W.W., Ross, D.C. and Marques, H.M., J. Inorg. Biochem., 68 (1997) 137.
24. Sullivan, D.J., Jr., Gluzman, I.Y., Russell, D.G. and Goldberg, D.E., Proc. Natl. Acad. Sci. USA, 93 (1996) 11865.
25. Sullivan, D. J., Jr., Matile, H., Ridley R.G. and Goldberg, D.E., J. Biol. Chem., 273 (1998) 31103.
26. Dorn, A., Vippagunta, S.R., Matile, H., Jaquet, C., Vennerstrom, J. L. and Ridley, R. G., Biochem. Pharmacol., 55 (1998) 727.
27. Orjih, A.U. and Fitch, C.D., Biochim. Biophys. Acta, 1157 (1993) 270.
28. Egan, T.J., Ross, D. C. and Adams, P.A., FEBS Lett., 352 (1994) 54.
29. Ursos, L.M.B., DuBay, K.F. and Roepe, P.D., Mol. Biochem. Parasitol., 112 (2001) 11.
30. Egan, T.J., Hempelmann, E. and Mavuso, W.W., J. Inorg. Biochem., 73 (1999) 101.
31. Foley, M. and Tilley, L., Pharmacol. Ther., 79 (1998) 55.
32. Hawley, S.R., Bray, P.G., Mungthin, M., Atkinson, J.D., O'Neill, P.M. and Ward, S.A., Antimicrob. Agents Chemother., 42 (1998) 682.
33. Egan, T.J. and Marques, H.M., Coord. Chem. Rev., 190–192 (1999) 493.
34. Egan, T.J., Exp. Opin. Ther. Patents, 11 (2001) 185.
35. Ziegler, J., Linck, R. and Wright, D.W., Curr. Med. Chem., 8 (2001) 171.
36. Winter, R.W., Cornell, K.A., Johnson, L.L., Ignatushenko, M., Hinrichs, D.J. and Riscoe, M.K., Antimicrob. Agents Chemother., 40 (1996) 1408.
37. Winter, R.W., Ignatushenko, M., Ogundahunsi, O.A.T., Cornell, K.A., Oduola, A.M.J., Hinrichs, D.J. and Riscoe, M.K., Antimicrob. Agents Chemother., 41 (1997) 1449.
38. Ignatushenko, M., Winter, R.W., Bachinger, H.P., Hinrichs, D.J. and Riscoe, M.K., FEBS Lett., 409 (1997) 67.
39. Ignatushchenko, M.V., Winter, R.W. and Riscoe, M.K., Am. J. Trop. Med. Hyg., 62 (2000) 77.
40. Vippagunta, S.R., Dorn, A., Matile, H., Battacharjee, A.K., Karle, J.M., Ellis, W.Y., Ridley, R.G. and Vennerstrom, J.L., J. Med. Chem., 42 (1999) 4630.
41. De, D., Krogstad, F.M., Byers, L.D. and Krogstad, D.J., J. Med. Chem., 41 (1998) 4918.
42. Egan, T.J., Hunter, R., Kaschula, C.H., Marques, H.M., Misplon, A. and Walden, J., J. Med. Chem., 43 (2000) 283.
43. De, D., Krogstad, F.M., Cogswell, F.B. and Krogstad, D.J., Am. J. Trop. Med. Hyg., 55 (1996) 579.
44. Ridley, R.G., Hofheinz, W., Matile, H., Jaquet, C., Dorn, A.O., Masciadri, R.O., Jolidon, S.O., Richter, W. F.O., Guenzi, A.O., Girometta, M., Urwyler, H., Huber, W., Thaithong, S. and Peters, W., Antimicrob. Agents Chemother., 40 (1996) 1846.
45. Battacharjee, A.K., J. Mol. Struct. (Theochem.), 529 (2000) 193.
46. Battacharjee, A.K., J. Mol. Struct. (Theochem.), 549 (2001) 27.
47. Battacharjee, A.K. and Karle, J.M., J. Med. Chem., 39 (1996) 4622.
48. Menezes, C.M.S., Sant'Anna, C.M.R., Rodrigues, C.R. and Barreiro, E.J., J. Mol. Struct. (Theochem.), 579 (2002) 31.
49. Kaschula, C.H., Egan, T.J., Hunter, R., Basilico, N., Parapini, S., Taramelli, D., Pasini, E. and Monti, D., J. Med. Chem., 45 (2002) 3531.
50. Hawley, S.R., Bray, P.G., O'Neill, P.M., Park, B.K. and Ward, S.A., Biochem. Pharm., 52 (1996) 723
51. Becke, A.D., J. Chem. Phys.I, 98 (1993) 5648.
52. Lee, C., Yang, W. and Parr, R., J. Phys. Rev. B, 37, (1998)785.
53. Hertwig, R.W. and Koch, W., J. Comput. Chem., 16 (1995) 576.
54. Jones, G., Willet, P. and Glen, R.C., J. Mol. Biol., 245 (1995) 43.
55. Jones, G., Willet, P., Glen, R.C., Leach, A.R. and Taylor, R., J. Mol. Biol., 267 (1997) 727.
56. Jones, G., Willet, P., Glen, R.C., Leach, A.R. and Taylor, R., ACS Symp. Ser., 719 (1999) 271.
57. Nissink, J.W.M., Murray, C., Hartshorn, M., Verdonk, M.L., Cole, J.C. and Taylor, R., Proteins, 49 (2002) 457.
58. Eldridge, M.D., Murray, C.W., Auton, T.R., Paolini, G.V. and Mee, R.P., J. Comput.-Aided Mol. Des., 11 (1997) 425.
59. Baxter, C.A., Murray, C.W., Clark, D.E., Westhead, D.R. and Eldridge, M.D., Proteins, 33 (1998) 367.
60. Bissantz, C., Folkers, G. and Rognan, D., J. Med. Chem., 43 (2000) 4759.
61. Schneider, G. and Bohm, H., Drug Discov. Today, 7 (2002) 64.
62. Beck, H.S. and Hardy, J., Proc. Natl. Acad. Sci. USA, 54 (1965) 286
63. Siegbahn, P., J. Am. Chem. Soc., 120 (1998) 8417.

64. Forrester, J. and Frisch, Æ, In Exploring Chemistry with Electronic Structure Methods, Gaussian, Inc., Pittsburgh, PA, 1996; pp. 64 and 157.
65. Fernandes, P.A. and Ramos, M.J., J. Am. Chem. Soc., 125 (2003) 6311.
66. Brooks, B.R., Bruccoleri, R.E., Olafson, B.D., States, D.J., Swaminathan, S. and Karplus, M., J. Comput. Chem., 4 (1983) 187.
67. MacKerell, A.D. Jr., Brooks, B., Brooks III, C.L., Nilsson, L., Roux, B., Won, Y. and Karplus, M., CHARMM: The Energy Function and Its Parameterization with an Overview of the Program, in The Encyclopedia of Computational Chemistry, 1, 271, P. v. R. Schleyer et al., Eds., John Wiley & Sons, Chichester, 1998.
68. Dewar, M.J.S., Zoebisch, E.G., Healy, E.F. and Stewart, J.J.P., J. Am. Chem. Soc., 107 (1985) 3902.
69. Voityuk, A.A. and Rösch, N., J. Phys. Chem. A, 104(17) (2000) 4089.
70. Adams, P.A., Berman, P.A.M., Egan, T.J., Marsh, P.J. and Silver, J., J. Inorg. Biochem., 63 (1996) 69.
71. Bauminger, E.R., Akkawi, M. and Blauer, G., Inorg. Chim. Acta, 286 (1999) 229.
72. Bohle, D.S., Debrunner, P., Jordan, P.A., Madsen, S.K. and Schulz, C.E., J. Am. Chem. Soc., 120 (1998) 8255.
73. Adams, P.A., Egan, T.J., Ross, D.C., Silver, J. and Marsh, P.J., Biochem. J., 318 (1996) 25.
74. Frisch, M.J., Trucks, G.W., Schlegel, H.B., Scuseria, G. E., Robb, M.A., Cheeseman, J.R., Zakrzewski, V.G., Montgomery, Jr., J.A., Stratmann, R.E., Burant, J.C., Dapprich, S., Millam, J.M., Daniels, A.D., Kudin, K.N., Strain, M.C., Farkas, O., Tomasi, J., Barone, V., Cossi, M., Cammi, R., Mennucci, B., Pomelli, C., Adamo, C., Clifford, S., Ochterski, J., Petersson, G.A., Ayala, P.Y., Cui, Q., Morokuma, K., Malick, D.K., Rabuck, A.D., Raghavachari, K., Foresman, J.B., Cioslowski, J., Ortiz, J.V., Baboul, A.G., Stefanov, B.B., Liu, G., Liashenko, A., Piskorz, P., Komaromi, I., Gomperts, R., Martin, R.L., Fox, D.J., Keith, T., Al-Laham, M.A., Peng, C.Y., Nanayakkara, A., Challacombe, M., Gill, P.M.W., Johnson, B., Chen, W., Wong, M.W., Andres, J.L., Gonzalez, C., Head-Gordon, M., Replogle, E.S. and Pople, J.A., Gaussian 98, Revision A.9, Gaussian, Inc., Pittsburgh, PA, 1998.
75. Portmann, S. and Lüthi, H.P., CHIMIA, 54 (2000) 766.
76. www.accelrys.com
77. Leach, A. R. Molecular Modelling: Principles and Applications (2nd Ed.), Prentice Hall, New York, 2001.
78. Portela, C., Afonso, C. M. M., Pinto, M. and Ramos, M. J., to be published.
79. Portela, C., Afonso, C. M. M., Pinto, M. and Ramos, M. J., FEBS Lett., 547 (2003) 217.